JCRS

Journal of Chemical Reactivity and Synthesis 2022: 12(3) 188-221

Research Article

Study of the effects of solvent and temperature on the Connections of the MTX and L-FMTX with Single-walled carbon nanotubes using QM and MM

Vahid Khodadadi[1], Neda Hasanzadeh[1*], Hooriye Yahyaei[2], Aye Rayatzadeh[1]

[1]Department of Chemistry, Ahvaz Branch, Islamic Azad University, Ahvaz, Iran
[2]Department of Chemistry, Zanjan Branch, Islamic Azad University, Zanjan, Iran

ARTICLE INFO:

Received:
1 July 2022

Accepted:
20 September 2022

Available online:
27 September 2022

✉: N. Hasanzadeh
nhzadeh_212@yahoo.com

ABSTRACT

In this study, using the density functional theory (DFT) computational methods and Monte Carlo simulation, the interaction of methotrexate (MTX) and its derivative (L-FMTX) with Single-walled carbon nanotubes (SWCNTS) was investigated. Through the DFT method, the effects of different solvents (water, methanol, ethanol, dimethyl sulfoxide and dimethylformamide) on the interaction of methotrexate (MTX) and its derivative (L-FMTX) with Single-walled carbon nanotubes within the Onsager self-consistent reaction field (SCRF) model, as well as the effects of temperature on the stability of interactions between compounds in various solvents were studied. The results showed that the MTX structure with the SWCNT single wall nanotube was more stable than the L-FMTX structure with SWCNT single wall nanotube. The results showed that the most stable solvent for the above-mentioned structures was water and that the most efficient force field was MM+.

Keywords: Single wall carbon nanotubes (SWCNT); methotrexate derivative (L-FMTX); methotrexate (MTX), self-consistent reaction field (SCRF); density functional theory (DFT)

1. Introduction

Nanoparticle drug delivery systems increase therapeutic efficacy in the face of the most severe cancer challenges, including drug resistance and tumor metastasis [1].

Nanoparticles are widely used in tissue engineering, targeted drug delivery and in the diagnosis of diseases. Nanoparticle drug delivery is one of the most practical aspects of cancer treatment and one advantage of targeted drug delivery is minimizing toxicity to normal, healthy cells[2-4].

Carbon nanotubes are a new form of pure carbon that consists of a hexagonal network of carbon atoms that form an integrated cylindrical tube. At both ends of the pipes there are caps of pentagonal carbon rings [5].

In the concentric shells structure, there is a 0.34 nm distance between the middle surfaces of every two shells. Single-walled carbon nanotubes consist of a rolled graphene plate, while multi-walled carbon nanotubes contain more than one concentric rolled graphene sheet. In other words, they have several shells that have an inner diameter of 0.4 nm [6].

Thus, a rolled sheet of graphene is called a single-walled carbon nanotube, a CNT with two sheets is called a double-walled carbon nanotube, and a CNT with three or more sheets is called a multi-walled nanotube [7, 8].

A carbon atom in a carbon nanotube has six electrons, two of which fill the s1 orbital and four of which fill the sp2 orbital. The rolled structure of carbon nanotubes causes σ-π hybridization in which three σ bonds are slightly off the surface, which causes the π orbital to be concentrated outside the nanotubes [9, 10].

Carbon nanotubes have many applications due to their unique properties; they are used as sensors [11], for gene therapy [12] and as drug nanocarriers [13].

Carbon nanotubes are classified into three types based on the direction of the roll: chair form, zigzag form and chiral form. Each of the three nanotube shapes can be created by rotating the nanotube along the vectors [14].

Carbon nanotubes can be used as transport carriers. In particular, they are able to cross cell membranes and also enter cell nuclei. In addition, these carbon nanotubes have suitable properties for becoming drug carriers. For example, they benefit from suitable internal empty spaces for the storage of drugs and biological materials. Moreover, carbon nanotubes have distinct internal and external surfaces that can be used separately for different purposes. For example, a drug or biological substance can be placed inside the CNT and biocompatible groups suitable for the intended purposes can be attached to the outer surface of the CNT [15].

The use of carbon nanotubes as drug carriers, in addition to increasing the effectiveness of the drug, reduces drug-induced toxicity and improves the pharmacological activity of biomolecules [16, 17]. As effective drug delivery systems, carbon nanotubes show good potential for cancer treatment [18].

Single-walled carbon nanotubes have shown a more effective role in drug delivery in cancer patients due to their unique physical and chemical properties and low toxicity. These nanotubes can bind covalently or non-covalently with different biological molecules. This complex is then absorbed by the organs inside the cell [19, 20].

The use of Single-walled carbon nanotubes causes a greater proportion of the drug entering the body to reach the cancer cells; this reduces the total amount of drug needed for injection and creates the desired therapeutic effect [21]. Studies have shown that compared to multi-walled nanotubes, smaller single-walled nanotubes can enter the cytoplasm and nuclei of cells and cross cell membranes more easily [22].

Therefore, these substances quickly became useful in various scientific fields, including medicine and drug delivery, where the play an important role in targeting cells in certain diseases such as cancers and tumors.

Methotrexate is a competitive inhibitor of the enzyme dihydrofolate reductase, preventing the conversion of dihydrofolate to tetrahydrofolate, which is essential for the synthesis of purines and pyrimidines. Methotrexate was first used to treat malignancies. Compared to the doses used to treat malignancies, much lower doses are used for cancer treatment [23]. Although it has low cellular uptake, Methotrexate is a drug that is widely used in the fight against cancer [24-26]. Combining Methotrexate with nanotubes which increases its internalization is a promising way to overcome its limited cellular uptake Methotrexate (MTX), with the molecular formula C20H22N8O5, is an anticancer drug with a folic acid-like structure as displayed in

Figure 1.

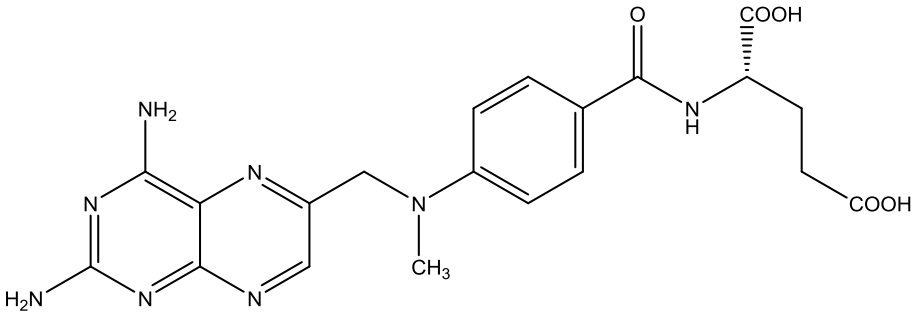

Figure 1. The Structure of Methotrexate

Methotrexate has several derivatives, each of which has unique characteristics and some of which also have medicinal properties. In this study, one of the fluorinated derivatives of methotrexate (Figure 2) as well as the complex obtained from the mentioned derivative with single-walled nanotubes was also investigated.

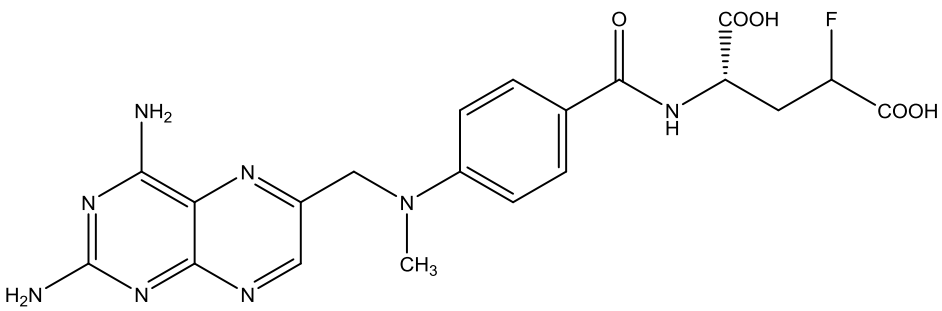

Figure 2. The Structure of γ -Fluoromethotrexate (L-FMTX)

The present study aims to investigate drug delivery systems using Single-walled carbon nanotubes and releasing the active drug at appropriate locations; it also investigates the theory behind the binding of methotrexate and its derivative to single-walled carbon nanotubes.

2. Computational method (Experimental)

One of the most common numerical techniques that is widely used in quantum mechanics, field theory, statistical physics, etc. is the Monte Carlo computational method [27].

The Monte Carlo method, which is a common method for simulating physical systems, is a computational-based algorithm based on the use of random sampling to calculate results. Monte Carlo-based algorithms are very useful in finding important combinations of flexible biomolecules due to their tendency to sample low-energy regions of structural spaces. The Monte Carlo simulation method shows the uncertainty quantitatively and explicitly. This method is a set of computational algorithms that relies on repetitive and random sampling to calculate the results. It is useful when systems have integrals that are difficult to solve and produce random numbers to find constant values [28-30].

The tendency to sample low-energy points of structural spaces is very important in Monte Carlo methods in finding structures and detecting, understanding and studying important compounds of biomolecules. Monte Carlo simulations are also used to understand the properties and structures of liquids, including estimating liquid density and evaporation heat. The advanced version of HyperChem software [31], which is one of the most common computational chemistry software in the field of quantum computing and in the computation of other physical properties of chemical molecules, was used to simulate Monte Carlo, optimize the geometric structure and perform molecular mechanical calculations in this study [32]. In addition to the possibility of drawing molecular structures and observing simulated systems in a three-dimensional environment, this software is also able to perform computational operations and simulate various chemical reactions.

The GAUSSIAN 09 software [33], which is one of the most powerful computational chemistry software, was also used to perform quantum chemical calculations The energy of the molecular structure of the existing compounds was optimized using the density functional theory (DFT) and with the basic method and set B3LYP /6-31+G* [34, 35].

In DFT, the electronic structure is evaluated using a potential function on the electrons of the system. In the theory of density citizenship, instead of the particle wave function (in quantum mechanics), the electron density function is used as the main factor in studying the physical properties of the system. This method is better, slightly more accurate, more complete and less time consuming [27].

Calculations related to fragment molecular orbitals (FMO) and thermodynamic parameters were performed through electron density citizenship theory ; in addition, the molecular properties of structures such as ionic potential (I), electron seeking (A), chemical hardness (η), electrochemical potential (μ) and electrophilicity (ω) were investigated [36-39].

In addition to DFT calculations, in this study the interaction of the methotrexate anticancer drug (MTX) and its derivative (L-FMTX) with Single-walled carbon nanotubes was examined by performing the corresponding Monte Carlo calculations using each of the AMBER [40], OPLS [41], CHARMM [42, 43] and MM+ [31] force fields: the difference between the force fields is shown by comparing the energies calculated using the stated force fields. This method was performed using the advanced HYPER CHEM software and by placing methotrexate and its derivative in Single-walled carbon nanotubes in the environment of this software.Choosing a force field that is well parameterized for the molecular system is very important [31, 44].

3. Results and discussion

Given that the formation of a stable complex between methotrexate and its derivative with drug nanocarriers is of particular importance, in this study the molecular structure and thermodynamic stability of the complex formed by the interaction between methotrexate and its derivative with a single-walled Zigzag model carbon nanotube were examined and compared.

In this study, the four force fields AMBER, OPLS, CHARMM and MM+ were used for molecular simulation; these force fields have been continuously developed and improved over time. Due to the tendency of Monte Carlo based algorithms to sample low energy areas of structural spaces, it is widely used in recognizing and studying compounds and biomolecules.

In Monte Carlo simulations, any system configuration can be generated randomly by moving a single atom or molecule. In some cases, a new configuration is created by moving multiple atoms or molecules or by rotating around one or more bonds. Therefore, the new configuration is calculated using the kinetic, potential and total energy functions.

The effect of different solvents and temperatures on methotrexate and its derivative with single-walled carbon nanotube (SWNT) – as a hybrid material – was investigated both through molecular mechanical simulation and by quantum mechanical calculations.

By comparing the kinetic, potentials and total energies calculated in AMBER, OPLS, CHARMM and MM+ force fields, the difference between the force fields is demonstrated; also, by using the GAUSSIAN 09 computer software and based on the base method and level B3LYP /6-31+G*, Quantum mechanical (QM) calculations were performed.

Using the Monte Carlo method, the energy of structures was first calculated in the gas phase and then in different solvents with various dielectric constants, including water, methanol, ethanol, DMSO and DMF at ten different temperatures in the temperature range of 298 K to 316 K. Then, the stability of the structures was also examined and compared in the same solvents and at the same temperatures mentioned above.

In the Monte Carlo method, sampling can be efficient, achieved through advanced structural search techniques. In addition, the experimental values of the predicted properties of a field represent its quality. The Total, potential and kinetic energies (in Kcal/Mol) were calculated for both structures in different solvents and various force fields, the results of which are listed in Tables to The Ekin changes (Kcal/Mol) calculated versus temperature at different dielectric constants of water ($\varepsilon = 78.39$), methanol ($\varepsilon = 32.63$), ethanol ($\varepsilon = 24.55$), DMSO ($\varepsilon = 46.8$) and DMF ($\varepsilon = 38.3$) are listed in Figures and Figures display the results of the Monte Carlo calculations .They show that in the AMBER force field, MTX and L-FMTX connected to SWCNT have the lowest amount of energy and are the most stable in the gas phase; however, among the solvents, methanol has the lowest amount of energy and is the most stable solvent for simulation.

Similar results were obtained for the OPLS and CHARMM force fields, but the best results were obtained from the calculations performed in the MM+ force field. Also, the results pointed to the lowest amount of energy in water, which was the best and the most stable solvent for simulation. Considering that the water solvent had the most distinctive and highest dielectric constant compared to the other solvents, it can be said that the energy and stability of a solvent are related to the dielectric constant. Polarization occurs easily in materials with high dielectric constant (such as water in this study).

According to Tables and Figures the results related to both MTX and L-MTX attached to a single-walled carbon nanotube correspond to each other. Among the solvents used, Methanol is the most stable in the OPLS and CHARMM force fields, but in the MM+ field, water was more stable than the other solvents.

Based on the energy diagrams obtained from Monte Carlo calculations, the potential energy is a key determiner of the changes in total energy in the stability or instability of the drug's bonding to the nanotube. Examining the diagrams, it is observed that as temperature increased, the potential energy drops. In other words, at higher temperatures, we see less potential energy and more stability, and this trend is similar in all the employed force fields. However, the calculations related to the MM+ force field yielded significant results. In this field, water was the most stable and suitable solvent among the studied solvents and had the lowest energy.

At certain temperatures and in some fields, such as OPLS and CHARMM, the methanol solvent had similar results and had good stability, but as mentioned before, in the MM+ force field, which is a specific field for macromolecule calculations, significant results were obtained. In some solvents, and at specific temperatures, the CHARMM force field exhibits similar behaviors to MM+ and stabilized the proposed composition.

The dielectric constant of a solvent (or relative permeability constant) is a quantity that demonstrates the ability of a solvent to separate pairs of positive and negative ions from each other. Solvents with high dielectric constants (like water) are easily polarized. Among the investigated solvents, water had the lowest energy and highest stability, and its dielectric constant was higher than the others. Furthermore, water is a biological solvent and acts as the main basis for chemical reactions, which can lead the simulation conditions to the most stable form. Comparing the energies in the force fields revealed that the lowest amount of energy was attributed to the MM + force field and water solvent at 316 K.

Table 1. The Total (Etot), Potential (Epot) and Kinetic (Ekin) energies (kcal/mol) calculated for the Native structure by Monte Carlo simulation in different solvents in theAmber force field (MTX with SWCNT).

Monte Carlo/Amber											
Temperature		**298K**	**300K**	**302K**	**304K**	**306K**	**308K**	**310K**	**312K**	**314K**	**316K**
Gas (εr =1)	E_{kin}	210.5211	211.934	213.3469	214.7598	216.1727	217.5856	218.9985	220.4114	221.8242	223.2371
	E_{pot}	4301.684	1360.168	1207.991	1124.592	1098.445	1045.906	1000.514	1012.418	988.9594	980.6787
	E_{tot}	4512.205	1572.102	1421.338	1339.352	1314.618	1263.491	1219.513	1232.83	1210.784	1203.916
Water (εr =78.39)	E_{kin}	1537.603	1547.923	1558.242	1568.562	1578.881	1589.201	1599.52	1609.84	1620.159	1630.479
	E_{pot}	7701.308	709.5659	-116.8135	-442.6804	-624.1889	-721.6329	-868.6838	-914.6525	-932.4508	-1039.732
	E_{tot}	9238.912	2257.489	1441.429	1125.882	954.6925	867.568	730.8366	695.1874	687.7085	590.7466
Methanol (εr =32.63)	E_{kin}	477.0035	480.2049	483.4062	486.6076	489.809	493.0103	496.2117	499.4131	502.6144	505.8158
	E_{pot}	112801.4	33888.25	15556.97	10541.14	9114.482	8576.853	8228.55	7881.339	7657.359	7512.184
	E_{tot}	113278.4	34368.45	16040.37	11027.74	9604.29	9069.863	8724.762	8380.752	8159.974	8017.999
Ethanol (εr =24.55)	E_{kin}	610.2447	614.3403	618.4359	622.5315	626.6271	630.7227	634.8183	638.9139	643.0095	647.1051
	E_{pot}	281503.2	76457.67	39578.41	22946.16	16460.72	14090.05	12896.09	12209.43	11716.03	11341.24
	E_{tot}	282113.5	77072.01	40196.85	23568.7	17087.35	14720.77	13530.9	12848.35	12359.04	11988.35
DMSO (εr =46.8)	E_{kin}	654.6584	659.0521	663.4458	667.8395	672.2332	676.6268	681.0205	685.4142	689.8079	694.2016
	E_{pot}	94663.39	30766.8	16673.69	11692.69	9523.045	8533.76	7976.714	7588.132	7277.142	7119.441
	E_{tot}	95318.05	31425.85	17337.14	12360.53	10195.28	9210.387	8657.734	8273.546	7966.95	7813.642
DMF (εr =38.3)	E_{kin}	743.4859	748.4757	753.4656	758.4554	763.4453	768.4351	773.4249	778.4148	783.4046	788.3945
	E_{pot}	97043.9	37585.27	18974.94	13170.48	11402.89	10852.21	10543.68	10300.64	10107.97	9994.243
	E_{tot}	97787.38	38333.75	19728.41	13928.94	12166.34	11620.65	11317.1	11079.06	10891.37	10782.64

Table 2. The Total (Etot), Potential (Epot) and Kinetic (Ekin) energies (kcal/mol) calculated for the Native structure by Monte Carlo simulation in different solvents in the OPLS force field (MTX with SWCNT).

Monte Carlo/ OPLS											
Temperature		**298K**	**300K**	**302K**	**304K**	**306K**	**308K**	**310K**	**312K**	**314K**	**316K**
Gas (εr =1)	E_{kin}	210.5211	211.934	213.3469	214.7598	216.1727	217.5856	218.9985	220.4114	221.8242	223.2371
	E_{pot}	4585.843	1424.573	937.0904	842.7628	782.4532	733.1329	720.3787	707.5767	682.9005	652.1961
	E_{tot}	4796.364	1636.507	1150.437	1057.523	998.6259	950.7185	939.3771	927.9881	904.7247	875.4332
Water (εr =78.39)	E_{kin}	1537.603	1547.923	1558.242	1568.562	1578.881	1589.201	1599.52	1609.84	1620.159	1630.479
	E_{pot}	33741.44	3208.032	1568.416	836.1907	361.7393	-13.73618	-285.0799	-488.8704	-680.5511	-867.0926
	E_{tot}	35279.04	4755.955	3126.659	2404.753	1940.621	1575.465	1314.44	1120.97	939.6083	763.3863
Methanol (εr =32.63)	E_{kin}	477.0035	480.2049	483.4062	486.6076	489.809	493.0103	496.2117	499.4131	502.6144	505.8158
	E_{pot}	124099	41566.57	21769.48	14609.36	12780.93	12221.92	11825.4	11589.35	11437.28	11353.56
	E_{tot}	124576	42046.77	22252.89	15095.96	13270.74	12714.93	12321.61	12088.76	11939.89	11859.37
Ethanol (εr =24.55)	E_{kin}	610.2447	614.3403	618.4359	622.5315	626.6271	630.7227	634.8183	638.9139	643.0095	647.1051
	E_{pot}	317949.9	85433.54	44548.75	27906.72	20335.59	17559.04	15627.43	14419.03	13417	11817.21
	E_{tot}	318560.1	86047.88	45167.18	28529.26	20962.22	18189.76	16262.25	15057.94	14060	12464.32
DMSO (εr =46.8)	E_{kin}	654.6584	659.0521	663.4458	667.8395	672.2332	676.6268	681.0205	685.4142	689.8079	694.2016
	E_{pot}	121998.1	36942.97	19157.97	13435.76	10908.04	9667.637	8992.501	8564.524	8328.571	8132.158
	E_{tot}	122652.8	37602.02	19821.42	14103.6	11580.27	10344.26	9673.521	9249.938	9018.378	8826.36
DMF (εr =38.3)	E_{kin}	743.4859	748.4757	753.4656	758.4554	763.4453	768.4351	773.4249	778.4148	783.4046	788.3945
	E_{pot}	126576.2	44258.07	21382.49	14617.55	13004.05	12356.65	11925.29	11635.41	11405.72	11253.18
	E_{tot}	127319.7	45006.54	22135.96	15376	13767.5	13125.08	12698.72	12413.83	12189.12	12041.58

Table 3. The Total (E tot), Potential (E pot) and Kinetic (E kin) energies (kcal/mol) calculated for the Native structure by Monte Carlo simulation in different solvents in the CHARMM force field (MTX with SWCNT).

Monte Carlo/ CHARMM											
Temperature		**298K**	**300K**	**302K**	**304K**	**306K**	**308K**	**310K**	**312K**	**314K**	**316K**
Gas (εr =1)	E_{kin}	210.5211	211.934	213.3469	214.7598	216.1727	217.5856	218.9985	220.4114	221.8242	223.2371
	E_{pot}	3502.408	1195.034	856.0377	756.7777	706.5104	668.7651	643.4429	620.9258	607.4563	571.1967
	E_{tot}	3712.929	1406.968	1069.385	971.5375	922.6831	886.3507	862.4414	841.3371	829.2805	794.4338
Water (εr =78.39)	E_{kin}	1537.603	1547.923	1558.242	1568.562	1578.881	1589.201	1599.52	1609.84	1620.159	1630.479
	E_{pot}	2167.736	-3391.008	-4206.12	-4507.294	-4638.172	-4704.273	-4799.169	-4932.309	-4972.383	-4970.701
	E_{tot}	3705.34	-1843.085	-2647.878	-2938.732	-3059.291	-3115.072	-3199.648	-3322.469	-3352.224	-3340.222
Methanol (εr =32.63)	E_{kin}	477.0035	480.2049	483.4062	486.6076	489.809	493.0103	496.2117	499.4131	502.6144	505.8158
	E_{pot}	91945.87	35008.59	16778.84	12003.34	10510.41	9787.134	9362.204	9127.205	8932.238	8592.72
	E_{tot}	92422.87	35488.8	17262.24	12489.95	11000.21	10280.14	9858.416	9626.618	9434.852	9098.536
Ethanol (εr =24.55)	E_{kin}	610.2447	614.3403	618.4359	622.5315	626.6271	630.7227	634.8183	638.9139	643.0095	647.1051
	E_{pot}	265655.2	70307.78	35446.18	21334.73	16740.28	14783.43	13513.86	12507.95	11403.35	10713.2
	E_{tot}	266265.4	70922.12	36064.61	21957.26	17366.91	15414.16	14148.68	13146.86	12046.36	11360.31
DMSO (εr =46.8)	E_{kin}	654.6584	659.0521	663.4458	667.8395	672.2332	676.6268	681.0205	685.4142	689.8079	694.2016
	E_{pot}	170582.2	39843.12	20086.03	13775.94	11572.64	10399.47	9823.251	9434.371	9080.567	8736.918
	E_{tot}	171236.9	40502.17	20749.48	14443.78	12244.88	11076.09	10504.27	10119.79	9770.375	9431.12
DMF (εr =38.3)	E_{kin}	743.4859	748.4757	753.4656	758.4554	763.4453	768.4351	773.4249	778.4148	783.4046	788.3945
	E_{pot}	103249.7	37293.97	21019.25	15074.97	13004.5	12350.34	11827.25	11477.62	11144.98	10867.57

Table 4. The Total (Etot), Potential (Epot) and Kinetic (Ekin) energies (kcal/mol) calculated for the Native structure by Monte Carlo simulation in different solvents in the MM+ force field (MTX with SWCNT).

Monte Carlo/ MM+											
Temperature		**298K**	**300K**	**302K**	**304K**	**306K**	**308K**	**310K**	**312K**	**314K**	**316K**
Gas (εr =1)	E_{kin}	210.5211	211.934	213.3469	214.7598	216.1727	217.5856	218.9985	220.4114	221.8242	223.2371
	E_{pot}	1500.161	901.4761	761.6816	712.8203	634.4072	601.9166	577.8038	569.9135	555.8868	556.8354
	E_{tot}	1710.682	1113.41	975.0285	927.5801	850.5799	819.5022	796.8022	790.3248	777.7111	780.0726
Water (εr =78.39)	E_{kin}	1537.603	1547.923	1558.242	1568.562	1578.881	1589.201	1599.52	1609.84	1620.159	1630.479
	E_{pot}	18254.24	11484.08	7683.593	5387.485	3839.653	3013.839	2323.27	2051.374	1738.824	1542.081
	E_{tot}	19791.84	13032.01	9241.836	6956.047	5418.534	4603.04	3922.79	3661.214	3358.983	3172.56
Methanol (εr =32.63)	E_{kin}	477.0035	480.2049	483.4062	486.6076	489.809	493.0103	496.2117	499.4131	502.6144	505.8158
	E_{pot}	94358.97	72576.55	58611.3	48843.72	41821.43	36500.55	32412.08	28870.78	26080.32	23705.96
	E_{tot}	94835.98	73056.76	59094.71	49330.33	42311.24	36993.56	32908.29	29370.19	26582.93	24211.78
Ethanol (εr =24.55)	E_{kin}	610.2447	614.3403	618.4359	622.5315	626.6271	630.7227	634.8183	638.9139	643.0095	647.1051
	E_{pot}	155252.2	120452.6	98101.16	83753.44	72193.42	63347.63	55520.07	49128.26	43928.58	39842.18
	E_{tot}	155862.4	121066.9	98719.6	84375.97	72820.04	63978.35	56154.89	49767.17	44571.59	40489.28
DMSO (εr =46.8)	E_{kin}	654.6584	659.0521	663.4458	667.8395	672.2332	676.6268	681.0205	685.4142	689.8079	694.2016
	E_{pot}	112582.2	84122.59	66509.9	55302.35	46937.72	40828.36	36085.03	32008.44	28733.31	26215.18
	E_{tot}	113236.8	84781.64	67173.35	55970.19	47609.96	41504.98	36766.05	32693.86	29423.12	26909.38
DMF (εr =38.3)	E_{kin}	743.4859	748.4757	753.4656	758.4554	763.4453	768.4351	773.4249	778.4148	783.4046	788.3945
	E_{pot}	79612.04	60252.73	48653.5	41296.18	36117.43	32031.92	28432.16	25607.77	23291.04	21318.94
	E_{tot}	80355.53	61001.2	49406.96	42054.63	36880.87	32800.36	29205.59	26386.18	24074.45	22107.33

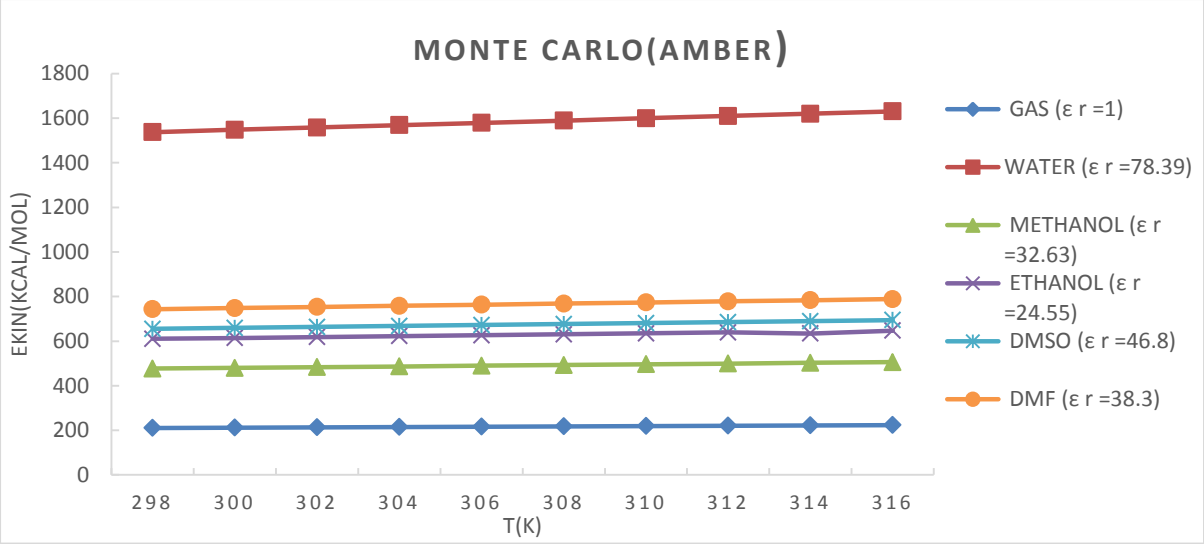

Figure 3. EKin changes (kcal/mol) calculated versus temperature at different dielectric constants through Monte Carlo simulation in the Amber force field for SWCNT with methotrexate.

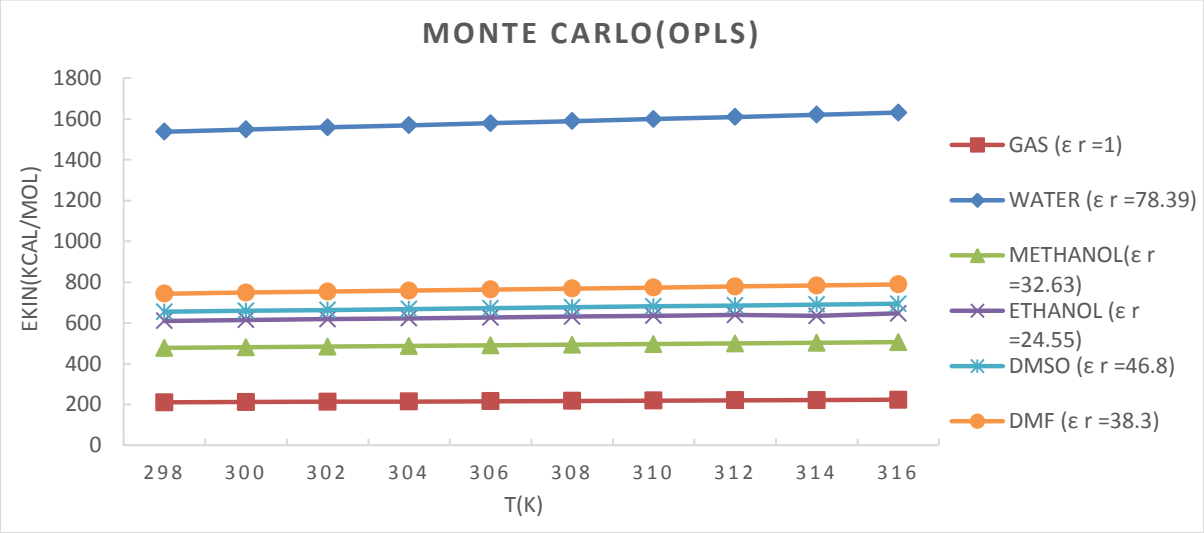

Figure 4. EKin changes (kcal/mol) calculated versus temperature at different dielectric constants through Monte Carlo simulation in the OPLS force field for SWCNT with methotrexate.

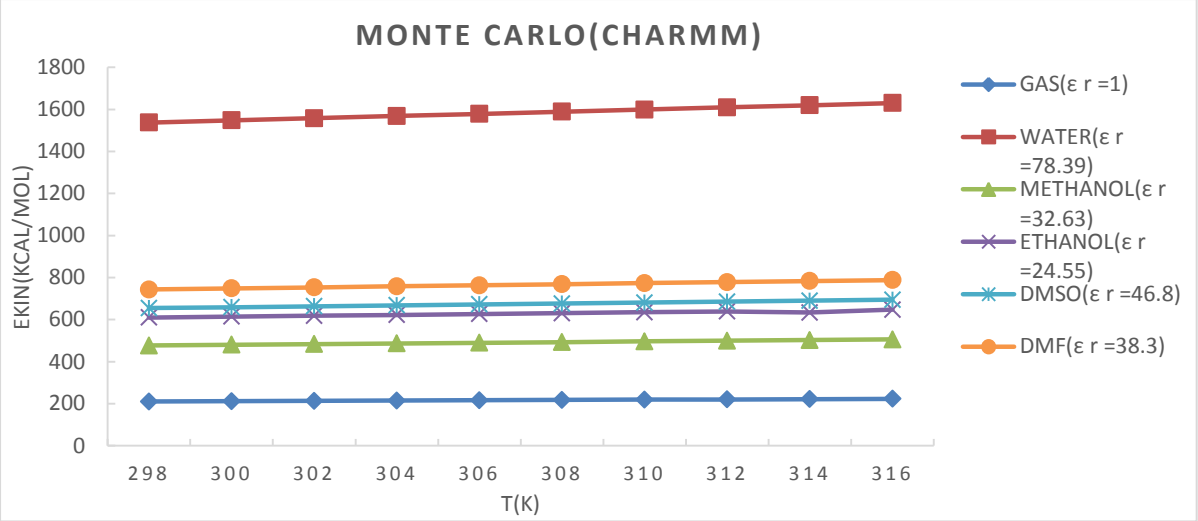

Figure 5. EKin changes (kcal/mol) calculated versus temperature at different dielectric constants through Monte Carlo simulation in the CHARMM force field for SWCNT with methotrexate.

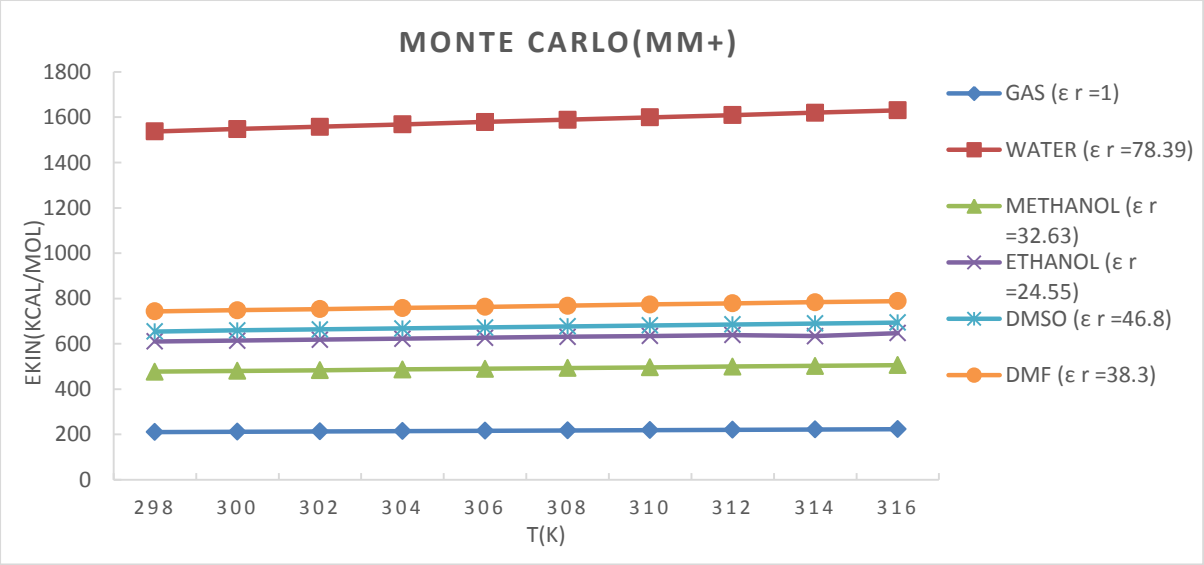

Figure 6. EKin changes (kcal/mol) calculated versus temperature at different dielectric constants through Monte Carlo simulation in the MM+ force field for SWCNT with methotrexate.

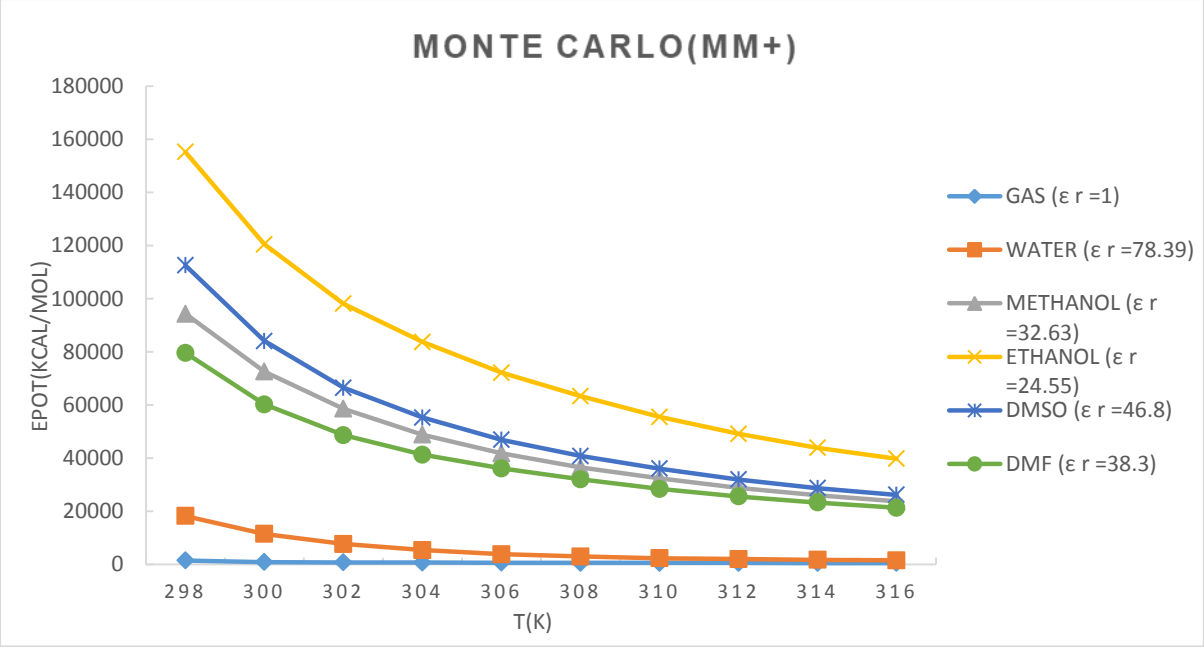

Figure 7. EPot changes (kcal/mol) calculated versus temperature at different dielectric constants through Monte Carlo simulation in the MM+ force field for SWCNT with methotrexate.

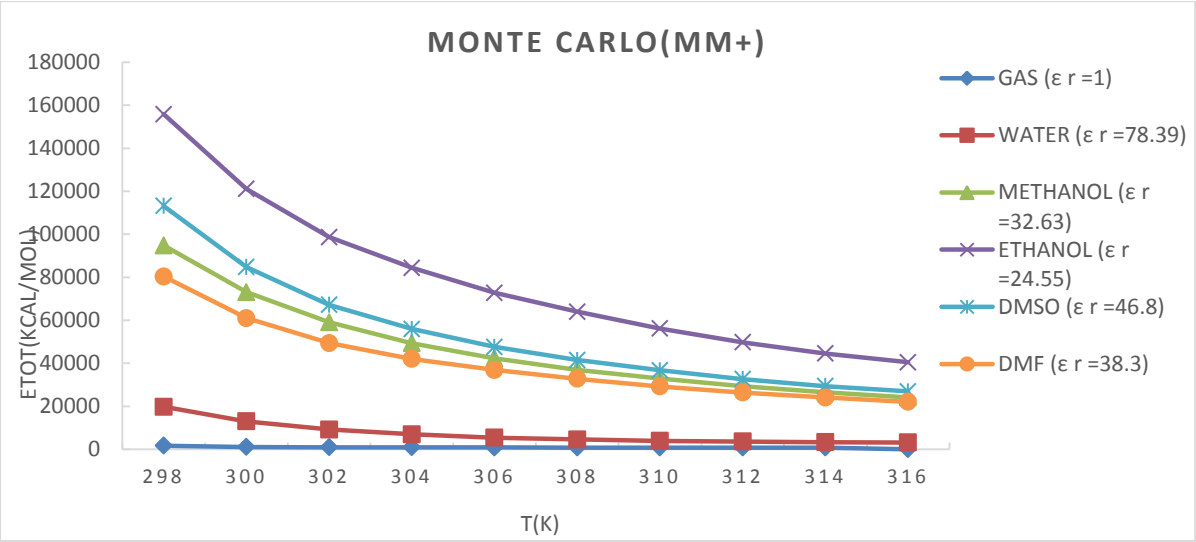

Figure 8. ETot changes (kcal/mol) calculated versus temperature at different dielectric constants through Monte Carlo simulation in the MM+ force field for SWCNT with methotrexate.

Table 5. The Total (Etot), Potential (Epot) and Kinetic (Ekin) energies (kcal/mol) calculated for the Native structure through Monte Carlo simulation in different solvents in the Amber force field (L-FMTX with SWCNT).

Monte Carlo/ Amber											
Temperature		**298K**	**300K**	**302K**	**304K**	**306K**	**308K**	**310K**	**312K**	**314K**	**316K**
Gas (εr =1)	E_{kin}	191.8673	193.155	194.4427	195.7304	197.0181	198.3058	199.5935	200.8812	202.1689	203.4566
	E_{pot}	2117.771	1225.532	1058.675	931.0661	933.2294	923.729	867.1447	878.7831	875.0392	869.306
	E_{tot}	2309.638	1418.687	1253.118	1126.796	1130.248	1122.035	1066.738	1079.664	1077.208	1072.763
Water (εr =78.39)	E_{kin}	1561.587	1572.067	1582.548	1593.028	1603.509	1613.989	1624.47	1634.95	1645.43	1655.911
	E_{pot}	3037.819	127.2017	-390.525	-627.0758	-812.1363	-968.6211	-1092.373	-1184.12	-1248.793	-1337.656
	E_{tot}	4599.406	1699.269	1192.023	965.9525	791.3724	645.3681	532.0967	450.8301	396.6372	318.2547
Methanol (εr =32.63)	E_{kin}	458.3497	461.4259	464.5021	467.5783	470.6544	473.7306	476.8068	479.8829	482.9591	486.0353
	E_{pot}	7059.326	2481.251	1939.663	1756.196	1607.393	1577.697	1534.902	1491.735	1440.843	1410.131
	E_{tot}	7517.676	2942.677	2404.165	2223.774	2078.047	2051.428	2011.709	1971.618	1923.802	1896.166
Ethanol (εr =24.55)	E_{kin}	591.5909	595.5613	599.5318	603.5022	607.4726	611.443	615.4134	619.3838	623.3542	627.3246
	E_{pot}	19485.37	6759.096	2833.553	2133.036	1768.255	1638.192	1523.055	1453.534	1368.77	1343.365
	E_{tot}	20076.96	7354.657	3433.084	2736.539	2375.728	2249.635	2138.468	2072.918	1992.125	1970.689
DMSO (εr =46.8)	E_{kin}	636.0047	640.2732	644.5416	648.8101	653.0786	657.3471	661.6156	665.8841	670.1526	674.4211
	E_{pot}	783098.7	158738.8	81668.91	46641.46	28838.85	21236.48	14625.12	17319.69	12341.05	10854.8
	E_{tot}	783734.7	159379	82313.45	47290.27	29491.93	21893.83	15291.01	17981.3	13011.21	11529.22
DMF (εr =38.3)	E_{kin}	724.8321	729.6968	734.5614	739.4261	744.2907	749.1554	754.02	758.8847	763.7493	768.6139
	E_{pot}	10019.44	6278.215	5716.09	5596.639	5505.949	5436.859	5362.967	5329.071	5308.406	5296.433
	E_{tot}	10744.27	7007.912	6450.651	6336.065	6250.24	6186.014	6116.987	6087.955	6072.155	6065.047

Table 6. The Total (Etot), Potential (Epot) and Kinetic (Ekin) energies (kcal/mol) calculated for the Native structure through Monte Carlo simulation in different solvents in the OPLS force field (L-FMTX with SWCNT).

Monte Carlo/ OPLS											
Temperature		**298K**	**300K**	**302K**	**304K**	**306K**	**308K**	**310K**	**312K**	**314K**	**316K**
Gas (εr =1)	E_{kin}	191.8673	193.155	194.4427	195.7304	197.0181	198.3058	199.5935	200.8812	202.1689	203.4566
	E_{pot}	1580.872	783.7602	592.4603	563.721	550.3422	538.3342	543.3423	508.8834	485.7192	488.6031
	E_{tot}	1772.739	976.9153	786.903	759.4514	747.3604	736.64	742.9358	709.7646	687.8881	692.0597
Water (εr =78.39)	E_{kin}	1561.587	1572.067	1582.548	1593.028	1603.509	1613.989	1624.47	1634.95	1645.43	1655.911
	E_{pot}	9773.001	1868.525	752.2815	101.7422	-330.9136	-606.6515	-843.575	-990.2384	-1114.59	-1237.073
	E_{tot}	11334.59	3440.592	2334.829	1694.77	1272.595	1007.338	780.8946	644.7116	530.8409	418.8377
Methanol (εr =32.63)	E_{kin}	458.3497	461.4259	464.5021	467.5783	470.6544	473.7306	476.8068	479.8829	482.9591	486.0353
	E_{pot}	32505.9	10558.25	7200.807	6553.31	6284.427	6166.538	6101.875	6033.602	5987.137	5978.359
	E_{tot}	32964.25	11019.68	7665.31	7020.889	6755.126	6640.269	6678.682	6513.485	6470.096	6464.394
Ethanol (εr =24.55)	E_{kin}	591.5909	595.5613	599.5318	603.5022	607.4726	611.443	615.4134	619.3838	623.3542	627.3246
	E_{pot}	64860.6	25523.51	15457.87	12249.07	9400.125	7896.721	7295.216	7086.083	6973.609	6857.047
	E_{tot}	65452.19	26119.07	16057.4	12852.58	10007.6	8508.164	7910.629	7705.467	7596.963	7484.371
DMSO (εr =46.8)	E_{kin}	636.0047	640.2732	644.5416	648.8101	653.0786	657.3471	661.6156	665.8841	760.1526	674.4211
	E_{pot}	1066973	171715.2	89045.46	52682.58	37365.09	29573.43	24107.06	20983.99	19450.03	18470.68
	E_{tot}	1067609	172355.5	89690	53331.39	38018.17	30230.78	24768.68	21649.87	20120.18	19145.1
DMF (εr =38.3)	E_{kin}	724.8321	729.6968	734.5614	739.4261	744.2907	749.1554	754.02	758.8847	763.7493	768.6139
	E_{pot}	85986.77	31142.27	18431.22	14878.56	13931.74	13371.66	13070.04	12824.04	12585.03	12441.69

Table 7. The Total (Etot), Potential (Epot) and Kinetic (Ekin) energies (kcal/mol) calculated for the Native structure through Monte Carlo Simulation in different solvents in the CHARMM force field (L-FMTX with SWCNT).

Monte Carlo/ CHARMM											
Temperature		**298K**	**300K**	**302K**	**304K**	**306K**	**308K**	**310K**	**312K**	**314K**	**316K**
Gas (εr =1)	E_{kin}	191.8673	193.155	194.4427	195.7304	197.0181	198.3058	199.5935	200.8812	202.1689	203.4566
	E_{pot}	2136.424	697.7448	551.223	523.3835	492.7575	469.0489	443.5285	480.121	426.2099	432.7651
	E_{tot}	2328.291	890.8999	745.6657	719.1139	689.7756	667.3547	643.1221	681.0022	628.3789	636.2217
Water (εr =78.39)	E_{kin}	1561.587	1572.067	1582.548	1593.028	1603.509	1613.989	1624.47	1634.95	1645.43	1655.911
	E_{pot}	-2145.394	-4392.597	-4686.699	-4842.167	-4997.402	-5074.476	-5135.178	-5223.327	-5271.585-	-5201.435
	E_{tot}	-583.8071	-2820.529	-3104.152	-3249.139	-3393.894	-3460.487	-3510.709	-3588.377	-3626.155	-3545.525
Methanol (εr =32.63)	E_{kin}	458.3497	461.4259	464.5021	467.5783	470.6544	473.7306	476.8068	479.8829	482.9591	486.0353
	E_{pot}	11468.88	3312.01	1679.971	1410.704	1308.615	1224.205	1164.526	1145.522	1131.006	1107.425
	E_{tot}	11927.23	3773.436	2144.473	1878.282	1779.269	1697.936	1641.332	1625.404	1613.965	1593.43
Ethanol (εr =24.55)	E_{kin}	591.5909	595.5613	599.5318	603.5022	607.4726	611.443	615.4134	619.3838	623.3542	627.3246
	E_{pot}	21506.33	9882.63	6236.548	5063.491	4806.418	4687.671	4640.72	4576.883	4549.721	4513.813
	E_{tot}	22097.92	10478.19	6836.08	5666.993	5413.891	5299.114	5256.133	5196.267	5173.075	5141.138
DMSO (εr =46.8)	E_{kin}	636.0047	640.2732	644.5416	648.8101	653.0786	657.3471	661.6156	665.8841	670.1526	674.4211
	E_{pot}	979668.4	198211.5	109812.7	67680.88	43963.16	30744.79	23202.24	20222.31	18405.9	17255.72
	E_{tot}	980304.4	198851.8	110457.3	68329.69	44616.23	31402.13	23863.85	20888.19	19076.05	17930.14
DMF (εr =38.3)	E_{kin}	724.8321	729.6968	734.5614	739.4261	744.2907	749.1554	754.02	758.8847	763.7493	768.6139
	E_{pot}	-43228.36	21901.32	13679.38	9668.724	8081.531	7595.775	7300.698	7055.506	6906.714	6811.584

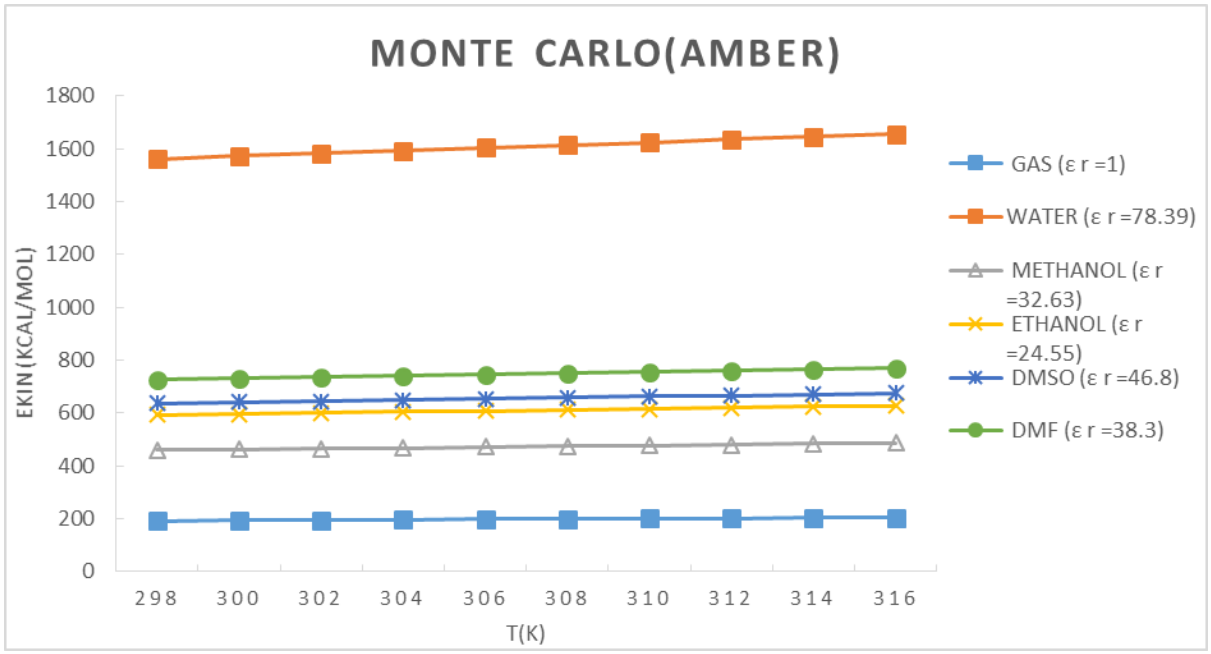

Figure 9. EKin changes (kcal/mol) calculated versus temperature at different dielectric constants through Monte Carlo simulation in the Amber force field for L-FMTX with SWCNT.

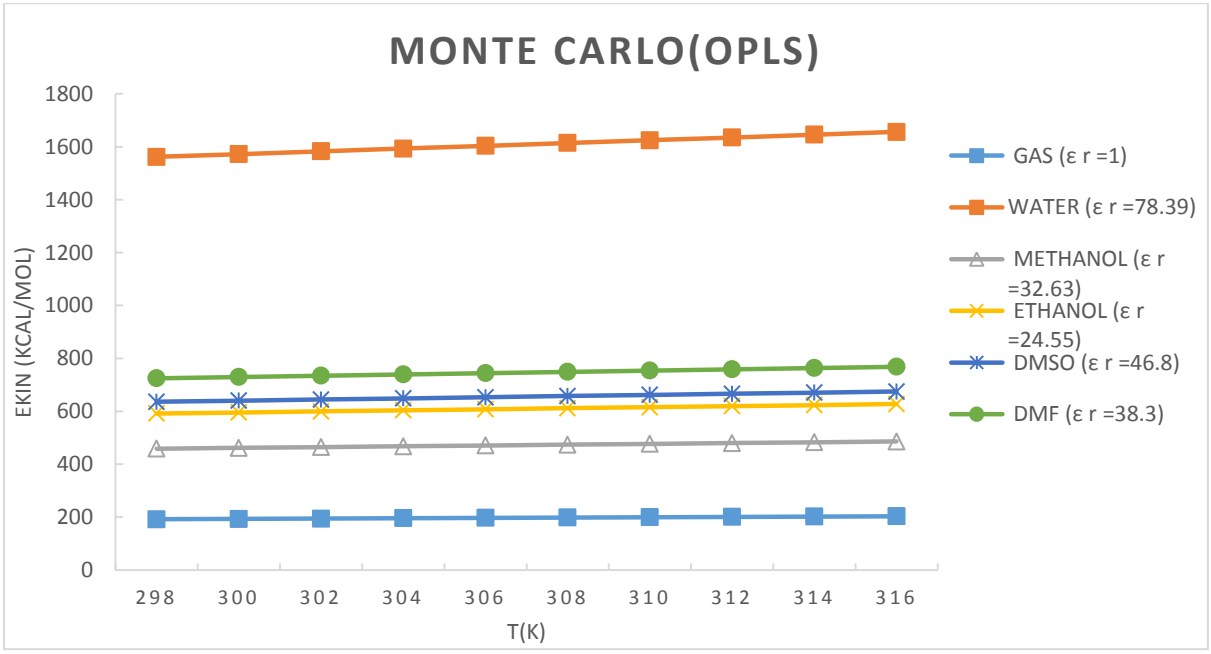

Figure 10. EKin changes (kcal/mol) calculated versus temperature at different dielectric constants through Monte Carlo simulation in the OPLS force field for L-FMTX with SWCNT.

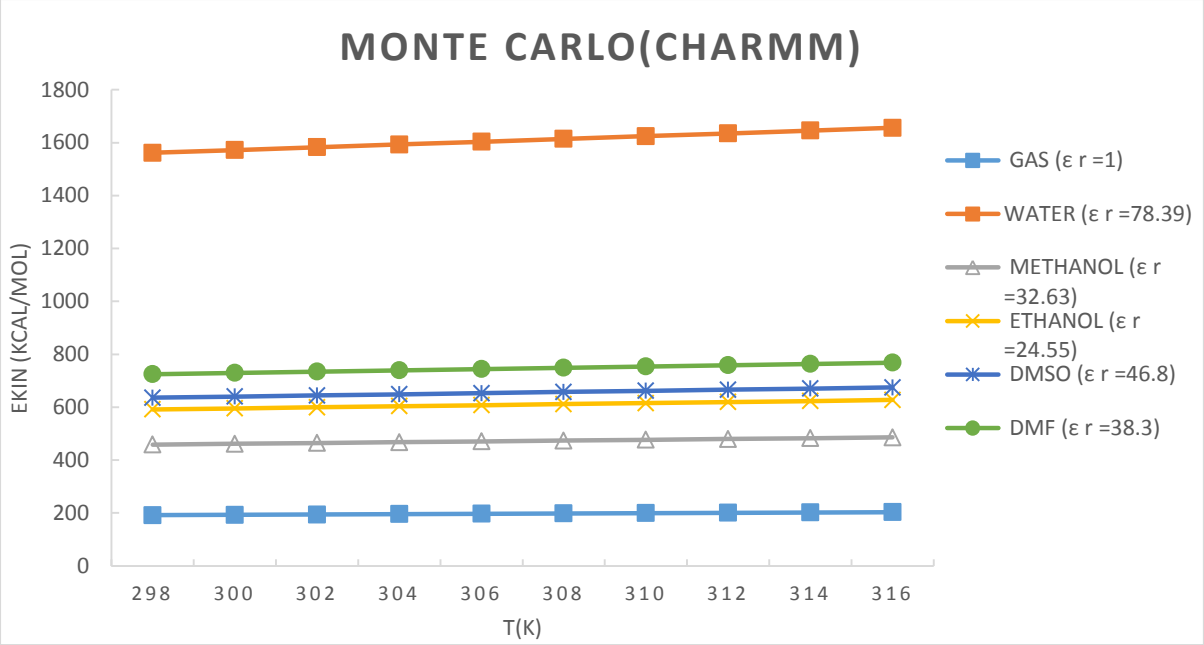

Figure 11. EKin changes (kcal/mol) calculated versus temperature at different dielectric constants through Monte Carlo simulation in the CHARMM force field for L-FMTX with SWCNT.

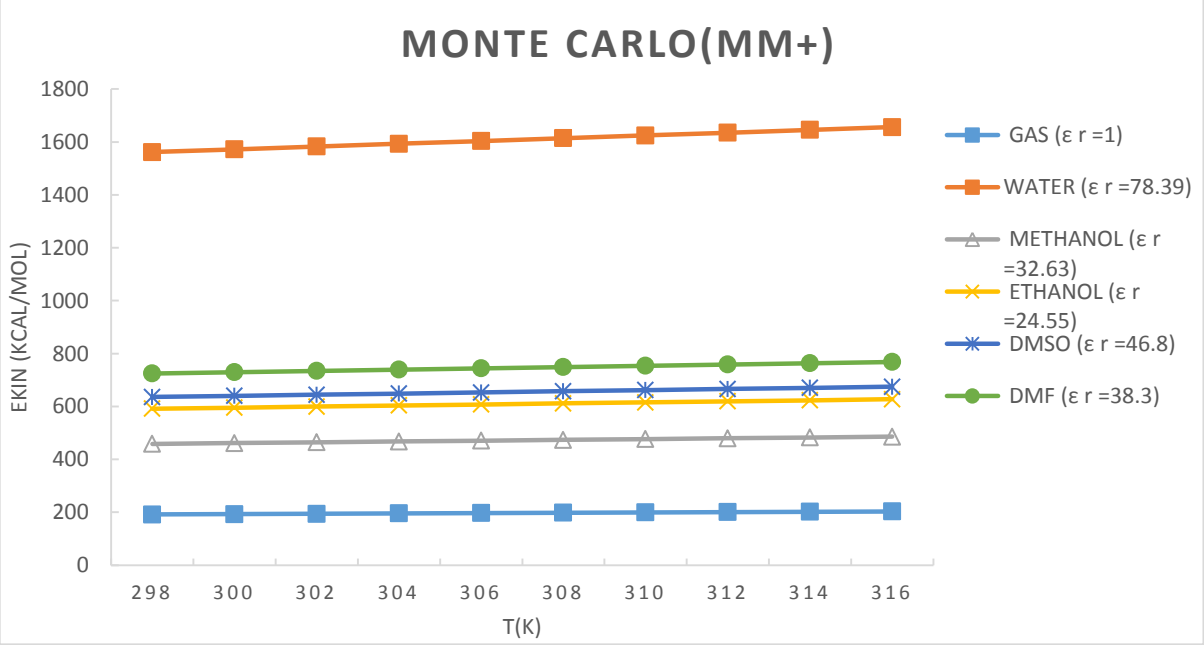

Figure 12. EKin changes (kcal/mol) calculated versus temperature at different dielectric constants through Monte Carlo simulation in the MM+ force field for L-FMTX with SWCNT.

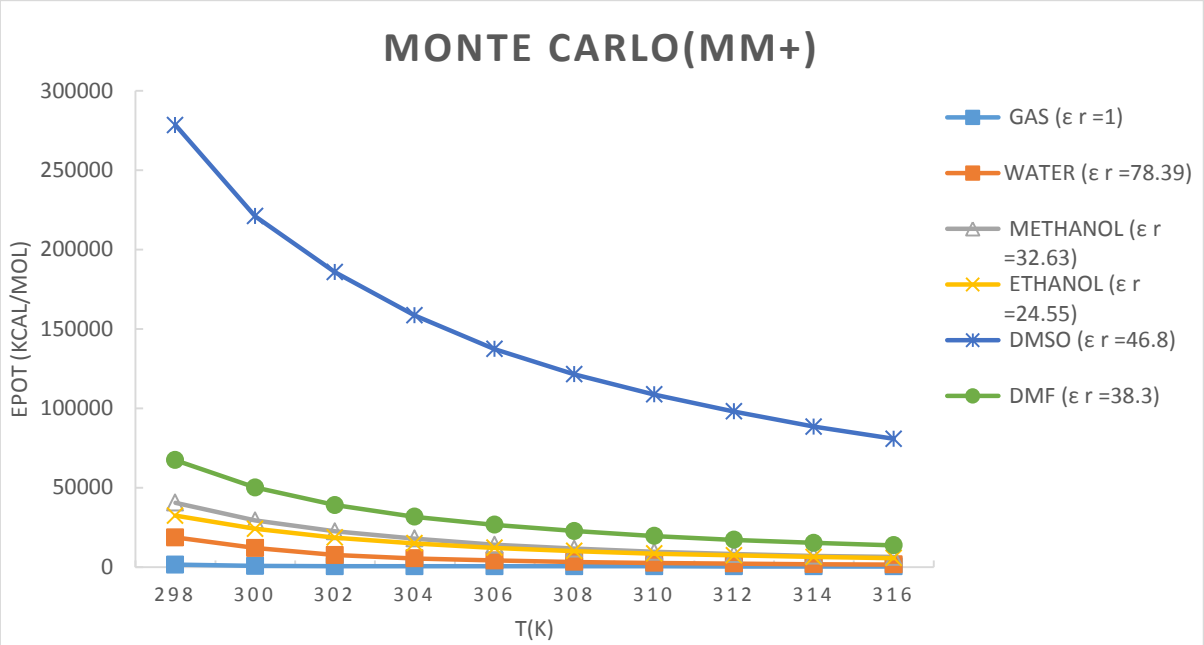

Figure 13. EPot changes (kcal/mol) calculated versus temperature at different dielectric constants through Monte Carlo simulation in the MM+ force field for L-FMTX with SWCNT.

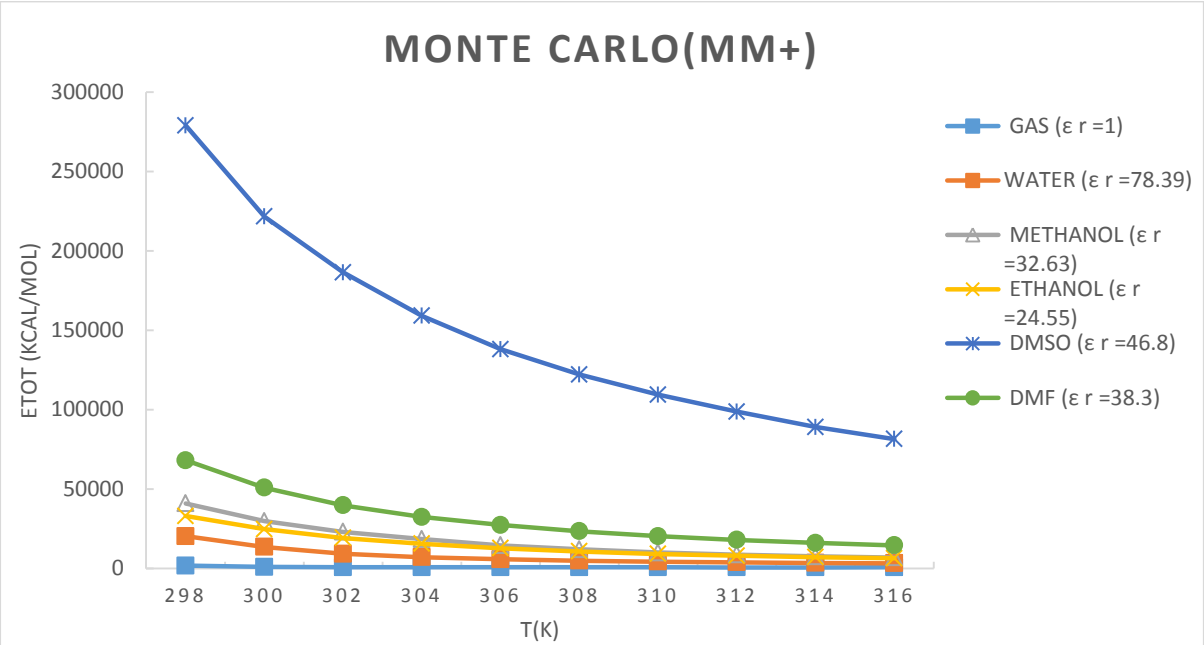

Figure 14. ETot changes (kcal.mol) calculated versus temperature at different dielectric constants through Monte Carlo simulation in the MM+ force field for L-FMTX with SWCNT.

Because in Monte Carlo simulations it is not possible to accurately reproduce thermodynamic properties such as heat capacity or vibrational entropy of isolated molecules, in this study the hybrid method of molecular mechanics and quantum mechanics was used. In this section, the calculations carried out through the Quantum Mechanics method will be examined:

Using quantum mechanics, which is one of the best methods for studying molecular structures and electrochemical behaviors, the energies of both structures (MTX and LFMTX) were initially optimized alone (without attachment to carbon nanotubes) and separately. Then, , molecular mechanical calculations related to each of the structures attached to the nanotubes, i.e. the structure of methotrexate attached to the single-walled carbon nanotube and also the structure of the methotrexate derivative attached to the single-walled carbon nanotube, were performed separately. In addition to obtaining the results related to boundary orbitals (FMO) such as EHOMO, ELUMO and gap energy (Δ ELUMO (- HOMO), thermodynamic parameters were calculated using the following equations:

$$(\eta = I - A/2) \quad (1)$$

$$(\chi = I + A/2) \quad (2)$$

$$(\mu = -(I + A)/2) \quad (3)$$

$$(\omega = \mu^2/2\eta) \quad (4)$$

$$(S = 1/2\eta) \quad (5)$$

All thermodynamic parameters obtained from the above equations including global hardness (η), electronegativity (χ), electrochemical potential (μ), electrophilicity (ω) and chemical softness (s) are reported.

According to the lowest energy is related to the structure of L-FMTX with SWCNT with the value -0.27820 eV. Due to the fact that the higher the slit energy, the less and slower the electron transfer, the large slit energy indicates a high stability for the molecule. Considering the HOMO-LOMO gap energy values (ΔE) obtained for MTX combinations with SWCNT and also L-FMTX with SWCNT, which are 0.018486 eV and 0.04198 eV, respectively, it is concluded that L-FMTX with SWCNT is more stable than MTX with SWCNT.

The value of chemical hardness (η) for the structure of MTX with SWCNT is η = 0.01927 eV; for the structure of L-FMTX with SWCNT, it is η = 0.02099 eV. The mentioned values indicate that the chemical hardness (η) of the L-FMTX with SWCNT is higher. Thus, this structure is less reactive than the other molecular structures and had more cleavage energy and more stability. As described above the higher energy gap of the L-FMTX structure with SWCNT (ΔE = 0.04198 eV) also confirms the stability of the aforementioned structure.

Table 9 shows that the amount of electron chemical potential (μ = - (I + A) / 2) that can be adsorbed or released during chemical reactions related to methotrexate with Single-walled carbon nanotubes is smaller (-0.01081eV).

The electrophilicity index (ω) provides information on electron transfer (chemical potential) as well as stability. Electrophilicity (ω = μ2 /2 η) is the energy stabilization criterion for when the system receives additional electrical charges from the environment. The higher the value of the electrophilic index, the greater the capacity of the molecule to accept electrons and, consequently, the greater the stability. The value of this index is 0.003032 eV for the MTX structure with SWCNT; for the L-FMTX structure with SWCNT, it is higher (1.575917 eV). Since the electrophilic index value of the L-FMTX with SWCNT is higher, its capacity for electron generation is very high.

The dipole moment (Debye) of molecules is a good indicator for evaluating their asymmetry. The higher the dipole moment of a molecule, the more asymmetric the structure of that molecule is. As shown in

all the structures have a high dipolar moment and have a point group C1 in terms of symmetric elements, which indicates that the structures are asymmetric.

Table 8. The electronic properties of the MTX and L-FMTX calculated using the B3LYP/6-31+G* level of theory.

The values of dipole moment for MTX with SWCNT and L-FMTX with SWCNT are 2.8990Debye and 0.5689 Debye, respectively. As can be seen, the bipolar torque value of the MTX with SWCNT is higher, indicating its asymmetric structure, and the more asymmetric the molecule, the less stable it is.

Table 9 shows the amount of Gibbs free energy for MTX with SWCNT (-313.7306032 Hartree) and the amount of Gibbs free energy for L-FMTX with SWCNT (-4967 113787 Hartree).

The lower (more negative) the amount of Gibbs free energy, the more stable that structure is. Here, too, the results show that the L-FMTX structure with SWCNT is more stable than the other structure. The greater stability of the L-FMTX structure with SWCNT is due to the presence of the element F with high electronegativity.

Density functional theory (DFT) calculations were performed in the gas phase [45-47]. The sum of the rotational, vibrational, transitional, and electronic energies is equal to the total energy of a molecule, and the total energy of a molecule is composed of the sum of these energies.

The thermochemical analysis is performed on the title compounds by placing the molecule at 25°C and at a pressure of 1 atmosphere. Thermodynamic parameters, such as rotational constant, zero point vibrational energy, entropy (S) and heat capacity (C) of the title compounds (using the level B3lyp/6-31+G*) are presented in table 8

According to this table, the values calculated for L-FMTX with SWCNT are smaller than those for the MTX with SWCNT. The results show that between the two structures, FMTX with SWCNT is more stable. DOS plots [48] also demonstrate the energy gaps (ΔE) calculated for the L-FMTX and MTX molecules

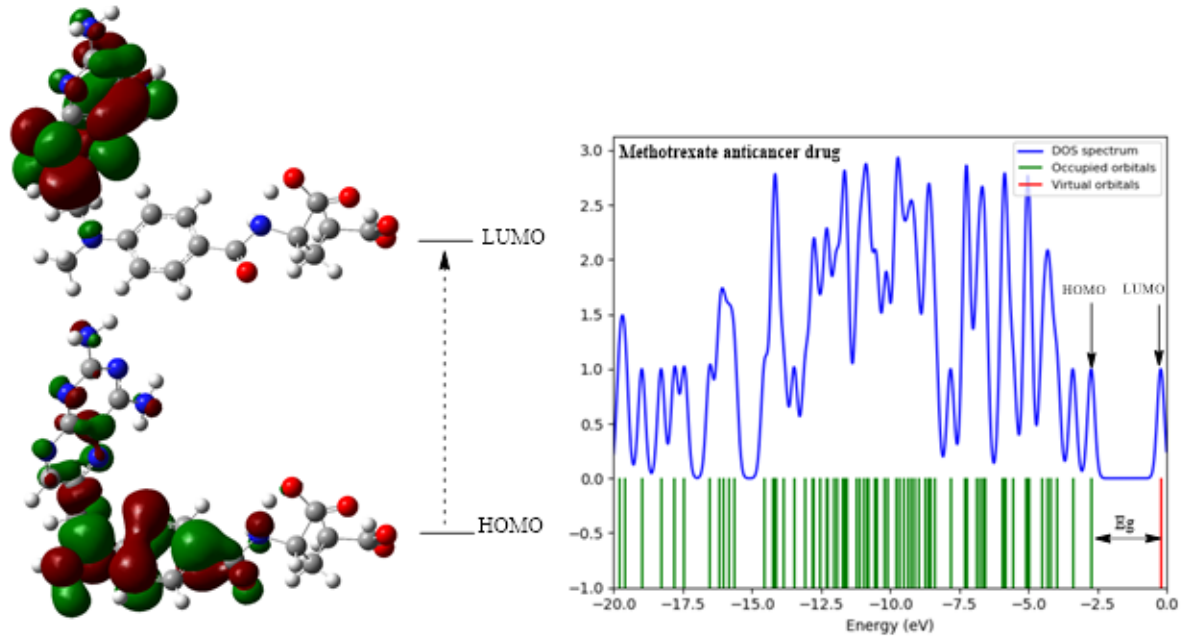

Figure 15. (a) Calculated Frontier molecular orbitals and (b) Calculated DOS [43] plots of Methotrexate (MTX) (ΔE: Energy gap between LUMO and HOMO), (using the B3lyp/6-31+G*).

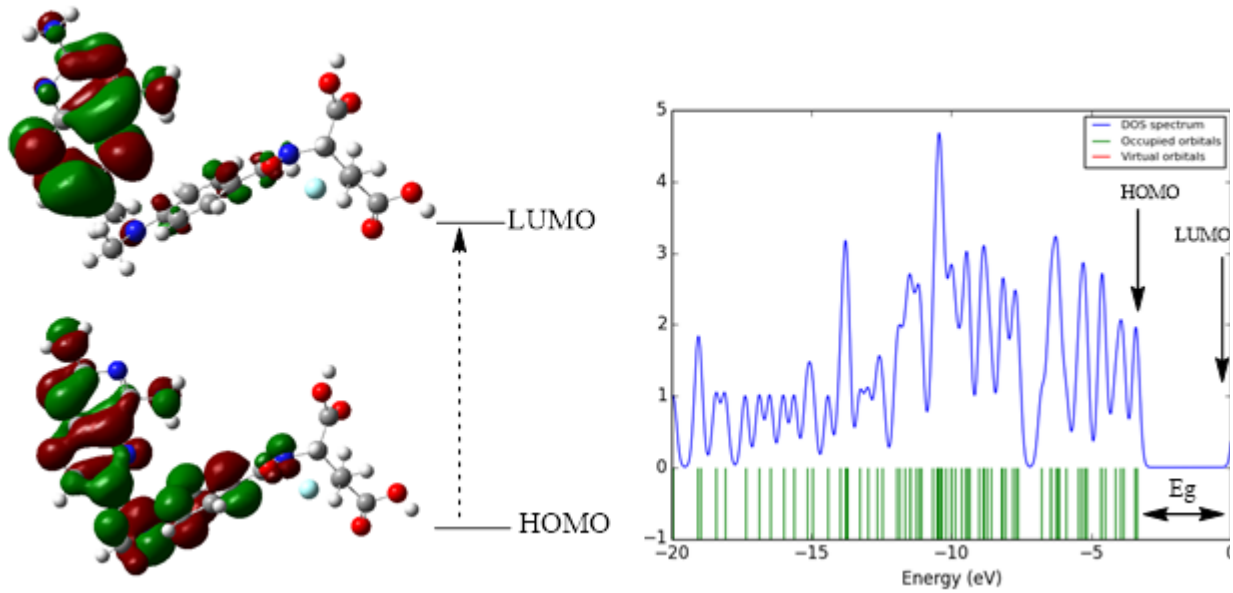

(a) **(b)**

Figure 16. (a) Calculated Frontier molecular orbitals and (b) Calculated DOS [43] plots of γ-Fluoromethotrexate (L-FMTX) (ΔE: Energy gap between LUMO and HOMO), (using the B3lyp/6-31+G*.

4. Conclusions

Conventional cancer control with chemotherapy drugs can have detrimental effects on healthy body tissues. As such, the use of drug nanocarriers to deliver anti-cancer drugs to the target organs or tissues and prevent damage to other healthy tissues is very promising.

In this study, the effects of solvents and different temperatures on MTX and L-FMTX anticancer drugs with SWCNT were investigated through quantum mechanical calculations and molecular mechanics simulations.

Monte Carlo simulation is one of the suitable and valuable methods for studying and understanding chemical structures. By comparing the energies calculated in the AMBER, OPLS, CHARMM (Bio+) and MM+ force fields, the difference between these fields was demonstrated.

When MTX bound to SWCNT was simulated in water, methanol, ethanol, DMSO and DMF, it was found that methanol had little energy and thus, was a stable solvent for simulation. Similar results were reported for OPLS and CHARMM fields. However, in the MM+ force field, the calculations performed showed a significant result. Based on the molecular simulation calculations performed and the studies carried out on the AMBER, OPLS, CHARMM and MM+ force fields, we found that MM+ is an exclusive and desirable field for macromolecular calculations. It has the lowest amount of energy and the most stable form of connection with MTX and L-FMTX with SWCNT. Therefore, the MM + was selected as the most efficient force field. Indeed, it should be pointed out that in some solvents and at specific field temperatures, The CHARMM force filed behaved similarly and stabilized our proposed composition.

Based on the results and graphs, it was observed that the energies are also affected by the dielectric constant of the solvent. The polarity of solvents also plays an important role in

calculating energies. The solvent's dielectric constant affects the interactions in solution that trap ions and polar molecules, and the intermolecular energy decreases as the dielectric constant rises. Water is the best solvent for drug simulation since it has the lowest amount of energy; in addition, it is a biological and non-toxic solvent and is not harmful to the body.

The observations and results of this study show that Single-walled carbon nanotubes are very important as a directional pharmaceutical source. In this study, the interaction of methotrexate and its derivative with single-walled carbon nanotube (SWCNT) was studied using DFT calculations in the gas phase. In general, methotrexate and its derivative have a stable connection with single-walled carbon nanotubes. However, the stability of L-FMTX with SWCNT is greater than that of MTX with SWCNT. The analysis of the obtained parameters showed that L-FMTX and single wall carbon nanotubes are more stable.

Finally, by controlling and slowing down the release of methotrexate and its derivatives and protecting drug molecules, and given their subcellular particle size, ability to cross biological barriers to deliver the drug to the target site, increased drug retention in the bloodstream, targeted drug delivery and biocompatibility, these nanostructures can be considered a very effective drug delivery system that increases the therapeutic efficacy of the drug.

Acknowledgment

The authors of this study thank the Islamic Azad University of Ahvaz and the Islamic Azad University of Zanjan for their partial support of this article.

References

[1] R. Sun, Y. Liu, S.-Y. Li, S. Shen, X.-J. Du, C.-F. Xu, Z.-T. Cao, Y. Bao, Y.-H. Zhu and Y.-P. Li, *Biomaterials*. 37 (2015) 405-414

[2] J. Shi, A.R. Votruba, O.C. Farokhzad and R. Langer, *Nano Lett.* 10 (2010) 3223-3230

[3] M.M. Omrani, M. Ansari and N. Kiaie, *Biointerface Research in Applied Chemistry*. 6 (2016) 1814-1820.

[4] Y. Zhou, K. Vinothini, F. Dou, Y. Jing, A.A. Chuturgoon, T. Arumugam and M. Rajan, *Arabian Journal of Chemistry*. 15 (2022) 103649

[5] S.S. Vedaei and E. Nadimi, *Appl. Surf. Sci.* 470 (2019) 933-942

[6] N. Anzar, R. Hasan, M. Tyagi, N. Yadav and J. Narang, *Sensors International*. 1 (2020) 100003

[7] K.E. Moore, D.D. Tune and B.S. Flavel, *Adv. Mater.* 27 (2015) 3105-3137

[8] M.M. Dahm, M.K. Schubauer-Berigan, D.E. Evans, M.E. Birch, J.E. Fernback and J.A. Deddens, *Annals of occupational hygiene*. 59 (2015) 705-723

[9] H. Qi, K. Teo, K. Lau, M. Boyce, W. Milne, J. Robertson and K. Gleason, *Journal of the Mechanics and Physics of Solids*. 51 (2003) 2213-2237

[10] L. Qu, F. Du and L. Dai, *Nano Lett.* 8 (2008) 2682-2687

[11] S. Saxena and A.K. Srivastava, *Carbon nanotube-based sensors and their application*, in *Nano-Optics*. Elsevier, **2020,** pp. 265-291.

[12] K. Bates and K. Kostarelos, *Adv. Drug Delivery Rev.* 65 (2013) 2023-2033

[13] S. Kumar, R. Rani, N. Dilbaghi, K. Tankeshwar and K.-H. Kim, *Chem. Soc. Rev.* 46 (2017) 158-196

[14] I.V. Zaporotskova, N.P. Boroznina, Y.N. Parkhomenko and L.V. Kozhitov, *Modern Electronic Materials*. 2 (2016) 95-105

[15] N. Sinha and J.-W. Yeow, *IEEE Trans. Nanobiosci.* 4 (2005) 180-195

[16] Z. Liu, K. Chen, C. Davis, S. Sherlock, Q. Cao, X. Chen and H. Dai, *Cancer research*. 68 (2008) 6652-6660

[17] J.-Y. Park, J.-S. Hyun, J.-G. Jee, S.J. Park and D. Khang, *International Journal of Nanomedicine*. 16 (2021) 4943-4957

[18] R.G. Mendes, A. Bachmatiuk, B. Büchner, G. Cuniberti and M.H. Rümmeli, *J. Mater. Chem. B.* 1 (2013) 401-428

[19] H. Dai, *Acc. Chem. Res.* 35 (2002) 1035-1044

[20] E. Dervishi, Z. Li, Y. Xu, V. Saini, A.R. Biris, D. Lupu and A.S. Biris, *Particulate Science and Technology*. 27 (2009) 107-125

[21] R.K. Jain and T. Stylianopoulos, *Nature reviews Clinical oncology*. 7 (2010) 653-664

[22] A. Elhissi, W. Ahmed, I.U. Hassan, V. Dhanak and A. D'Emanuele, *J. Drug Delivery*. 2012 (2012)

[23] S. Ayyappan, N. Sundaraganesan, V. Aroulmoji, E. Murano and S. Sebastian, *Spectrochimica Acta Part A: Molecular and Biomolecular Spectroscopy*. 77 (2010) 264-275

[24] M.A. Abdel-Reheim, A.A. Ashour, M.A. Khattab and A.G.A. Gaafar, *Journal of Applied Pharmaceutical Science*. 12 (2022) 129-141

[25] S. Jiang, L. Chang, J. Luo, J. Zhang, X. Liu, C.-Y. Lee and W. Zhang, *Analyst*. 146 (2021) 6170-6177

[26] E. Türk, M. Güvenç, M. Cellat, A. Uyar, M. Kuzu, A.G. Ağgül and A. Kırbaş, *Drug Chem. Toxicol.* 45 (2022) 1054-1065

[27] M. Kastner, *Commun. Nonlinear Sci. Numer. Simul.* 15 (2010) 1589-1602

[28] W.K. Hastings, *Biometrika*. 57 (1970) 97-109

[29] J.S. Liu, F. Liang and W.H. Wong, *J. Am. Stat. Assoc.* 95 (2000) 121-134

[30] H. Yahyaei and M. Monajjemi, *Fuller. Nanotub. Carbon Nanostructures*. 22 (2014) 346-361

[31] R. HyperChem, *7.0 for windows, Hypercube*. 2002, Inc.

[32] C. Sun, J.S. Lee and M. Zhang, *Adv. Drug Delivery Rev.* 60 (2008) 1252-1265.

[33] M. Frisch, G. Trucks, H. Schlegel, G. Scuseria, M. Robb, J. Cheeseman, G. Scalmani, V. Barone, B. Mennucci and G. Petersson, *Wallingford, CT*. 32 (2009) 5648-5652.

[34] C. Lee, W. Yang and R.G. Parr, *Phys. Rev. B: Condens. Matter*. 37 (1988) 785

[35] B. Johnson, J. Seminario and P. Politzer, *Modern Density Function Theory: A Tool for Chemistry*. 1995, Elsevier, Amsterdam.

[36] J. Tomasi, B. Mennucci and R. Cammi, *Chem. Rev.* 105 (2005) 2999-3094

[37] S. Shahab, M. Sheikhi, L. Filippovich, E. Dikusar, H. Yahyaei, R. Kumar and M. Khaleghian, *J. Mol. Struct.* 1157 (2018) 536-550

[38] H. Yahyaei, S. Sharifi, S. Shahab, M. Sheikhi and M. Ahmadianarog, *Lett. Org. Chem.* 18 (2021) 115-127

[39] S. Shahab, M. Sheikhi, L. Filippovich, R. Kumar, E. Dikusar, H. Yahyaei and M. Khaleghian, *J. Mol. Struct.* 1148 (2017) 134-149

[40] W. Cornell, P. Cieplak, C.I. Bayly, I.R. Gould and J. Merz, *J. Am. Chem. Soc*. 117 (1995) 5179-5197

[41] W.L. Jorgensen and J. Tirado-Rives, *J. Am. Chem. Soc*. 110 (1988) 1657-1666

[42] A.D. MacKerell Jr, D. Bashford, M. Bellott, R.L. Dunbrack Jr, J.D. Evanseck, M.J. Field, S. Fischer, J. Gao, H. Guo and S. Ha, *J. Phys. Chem. B*. 102 (1998) 3586-3616.

[43] E. Neria, S. Fischer and M. Karplus, *The Journal of chemical physics*. 105 (1996) 1902-1921.

[44] H. Yahyaei, M. Monajjemi, H. Aghaie and K. Zare, *J. Comput. Theor. Nanosci*. 10 (2013) 2332-2341

[45] N. Shajari and H. Yahyaei, *physical chemistry research*. 8 (2020) 705-718.

[46] H. Yahyaei, S. Shahab, M. Sheikhi, L. Filippovich, H.A. Almodarresiyeh, R. Kumar, E. Dikusar, M.Y. Borzehandani and R. Alnajjar, *Spectrochimica Acta Part A: Molecular and Biomolecular Spectroscopy*. 192 (2018) 343-360

[47] V. Khodadadi, N. Hasanzadeh, H. Yahyaei and A. Rayatzadeh, *J. Chil. Chem. Soc.* 66 (2021) 5365-5379

[48] A.D. Mackerell Jr, M. Feig and C.L. Brooks III, *J. Comput. Chem.* 25 (2004) 1400-1415.